Structural Engineering and Mechanics, Vol. 24, No. 5 (2006) 601-620
DOI: http://dx.doi.org/10.12989/sem.2006.24.5.601

An effective stiffness model for RC flexural members

Robertas Balevičius†

Laboratory of Numerical Modelling, Vilnius Gediminas Technical University, Sauletekio av. 11, LT-10223 Vilnius, Lithuania

(Received September 6, 2005, Accepted June 29, 2006)

Abstract. The paper presents an effective stiffness model for deformational analysis of reinforced concrete cracked members in bending throughout the short-term loading up to the near failure. The method generally involves the analytical derivation of an effective moment of inertia based on the smeared crack technique. The method, in a simplified way, enables us to take into account the non linear properties of concrete, the effects of cracking and tension stiffening. A statistical analysis has shown that proposed technique is of adequate accuracy of calculated and experimental deflections data provided for beams with small, average and normal reinforcement ratios.

Keywords: RC cross section; effective moment of inertia; cracking; tension stiffening.

1. Introduction

Reinforced concrete is a composite multi-factor nature material with nonlinear relations between stress and strain in compression as well as nonlinear bonding behavior of concrete and steel in tension inducing the strain-dependent tension stiffening effect. All these properties have to be modeled on the material level in order to be later homogenized by a suitable integration technique to the structural level. Hence, for detailed insight into the deformational response of RC structures, a civil engineer must choose between analytical, numerical or traditional code methods.

Numerical techniques which recently have rapidly progressed are based on the universal principles and provide great possibilities to apply sophisticated mathematical models. The main limitations of numerical methods are related to numerical errors and computational capabilities in application to large structures. The implementation of the efficient solution techniques to achieve convergence, which can have a crucial influence on the obtained results, is also strongly needed. Normally, the non linear equations are solved numerically using an incremental step-by-step Newton-type procedure. Furthermore, in a general case, the problem of analysis of reinforced concrete elements under short- or long-term loading is non-smooth and non-convex and has multiple solutions, i.e., several stress and strain states may correspond to the same load condition. This can even occur if stress-strain relationships used for concrete and reinforcing steel have no descending branches (e.g., Balevičius and Simbirkin 2005). Therefore, conventional iterative methods of the Newton-type are frequently inefficient when solving a set of non linear equations for reinforced concrete structures and do not allows us to find all possible solutions to the problems.

† Associate Professor, E-mail: robertas.balevicius@st.vtu.lt

The application of analytical methods to the analysis of RC structures is limited by a constitutive law of traditional mathematics, stating in particular, that the explicit solution in terms of radicals for polynomial equations of a degree greater than four do not exist. Therefore, in part, in developing the code methods have been usually used a great number of empirical expressions and non-physical factors. The code approaches (e.g., SNiP 1988, ACI 1999, prEN 2001, etc.) are presented in the analytical form and simple to use, but, actually, they are empirical and, in many cases, do not reveal the actual stress strain state, but ensure the safe design. However, code methods usually give statistically more accurate deflection results to experimental tests data than deflections obtained in numerical analysis based on modern multi-parameter material models (e.g., Kaklauskas 2004).

Numerical modelling of plain and reinforced concrete started in the late 1960s with the landmark papers of Rashid (1968), Ngo and Scordelis (1967) proposing the smeared and discrete crack models. In the sequel, various developments, such as shear retention factor (Suidan and Schnobrich 1973), tension stiffening/softening, fracture energy concepts (e.g., Pietruszczak and Mroz 1981, Bazant and Oh 1984, etc.), rate-dependent smeared crack models (e.g., Sluys and de Borst 1996, etc.) have been opened to discussion. A comprehensive overview and analysis of these methods was done by de Borst (2002).

The calculation of moment-curvature diagrams for a particular section of beam-column is usually an intermediate step before determining its load-deflection behavior, load-carrying capacity, and failure mode under a particular set of loads and boundary conditions in engineering technique. The extensive analytical and experimental studies of load-deflection responses of RC beams and columns have been reported since the 1960s. These methods comprise the analytical approaches of the complex evaluation of tensile concrete, crack depths and bond-slipping (e.g., Rozenbliumas 1966) as well as the simple estimates of the flexural rigidity of RC beam (e.g., Gilbert 1983, Chan *et al*. 2000), techniques involving an adjustment to the stiffness of the tensile steel for account the tension stiffening (e.g., Zalesov *et al*. 1988, Scott and Beeby 2005) and applications of unloading stress-strain diagram for tensile concrete (e.g., Lin and Scordelis 1975, Prakhya and Morley 1990, Kwak and Kim 2002, Kaklauskas 2004, etc.). The procedures of numerical analysis in application to large structures with many degrees of freedom can be simplified when analytical moment-curvature relationships are approximately known in advance. This approach has been implemented by Mendis and Darval (1988) determining the buckling functions of column in nonlinear analysis of softening frames. Rather than using the layer approach, the accompanying sophisticated calculations in the nonlinear analysis such as the determination of neutral axis and change of elastic stiffness, the authors incrementally revised the previously determined RC section moment-curvature relation considering the bond slipping effect (Kwak and Kim 2002). This methodology has been also focussed on the simplified finite elements modelling and analytical solutions.

Probably the best known method based on empirical equation of an effective moment of inertia and specified for many years in many codes of practice for simplified deflection calculations has been proposed by Branson (1968). This attractive conception has been studied and revised by various investigators. The influence of load types on the effective moment of inertia has been investigated by Al-Zaid *et al.* (1991) developing the model that estimates any type of a symmetrical loading. Mathematical representation of the probability of crack occurrence by the ratio between the area of the moment diagram of cracked section and the total area of the moment diagram for any loading has been provided as the basis for the calculation of the effective moment of inertia by Ning *et al*. (2001). Recently, the rational models for the effective moment of inertia have been developed for fiber-reinforced polymer-RC beams (Razaqpur and Isgor 2003, Yost *et al.* 2003).

This paper presents a method for deformational analysis of cracked RC flexural members based on the constitutive laws for materials and classical principles of the strength of materials. The method generally involves an analytical derivation of the effective moment of inertia which, in a simplified way, enables us to take into account the non linear properties of concrete, the effects of cracking and tension stiffening. The engineering applicability of proposed concept is verified by extensive comparison of analytical results with experimental data.

2. Stress strain state formulation

2.1 Basic assumptions

The present method is based on the following assumptions about the behavior of flexural RC members:

- Euler-Bernouilli's hypothesis of linear distribution of strains within the depth of cross section;
- A smeared crack approach;
- Perfect bond between reinforcement and concrete (reinforcement slippage occurring concrete cracking is included into unloading stress strain relationship for tensile concrete);
- All the fibres in the tensile zone satisfy the same stress strain law. Similarly, this is also valid to fibres of concrete in compression.
- Shear forces do not significantly affect stress state and stiffness of the element cross section and can be omitted.

2.2 Governing geometry and equilibrium relations

Based on the above assumptions, let us consider a statically determined non-prestressed beam as doubly reinforced concrete element under bending only (Fig. 1). Using the requirements of strain compatibility and denoting the stresses and strains by subscripts *c*/*ct* and *s*/*s*1 for compressive/ tensile concrete and for compressive/tensile reinforcements, the equilibrium equations can be expressed in this way:

$$\begin{cases} M_c + M_{ct} + M_{s1} + M_s = M \\ F_c - F_{ct} + F_{s1} - F_s = 0 \end{cases} \tag{1}$$

where:
$$M_c + M_{ct} = \frac{1}{\rho^2}\left(\sum_{j=1}^{k_c} \int_{\varepsilon_c^{j-1}}^{\varepsilon_c^{j}} b(y)\varepsilon_c \sigma_c(\varepsilon_c) d\varepsilon_c + \sum_{j=1}^{k_{ct}} \int_{\varepsilon_{ct}^{j-1}}^{\varepsilon_{ct}^{j}} b(y)\varepsilon_{ct} \sigma_{ct}(\varepsilon_{ct}) d\varepsilon_{ct} \right) \tag{1a}$$

$$M_{s1} + M_s = \sigma_{s1}(\varepsilon_{s1})(x - a_1)A_{s1} + \sigma_s(\varepsilon_s)(h_0 - x)A_s \tag{1b}$$

$$F_c - F_{ct} = \frac{1}{\rho}\left(\sum_{j=1}^{k_c} \int_{\varepsilon_c^{j-1}}^{\varepsilon_c^{j}} b(y)\sigma_c(\varepsilon_c) d\varepsilon_c - \sum_{j=1}^{k_{ct}} \int_{\varepsilon_{ct}^{j-1}}^{\varepsilon_{ct}^{j}} b(y)\sigma_{ct}(\varepsilon_{ct}) d\varepsilon_{ct} \right) \tag{1c}$$

$$F_{s1} - F_s = \sigma_{s1}(\varepsilon_{s1})A_{s1} - \sigma_s(\varepsilon_s)A_s \tag{1d}$$

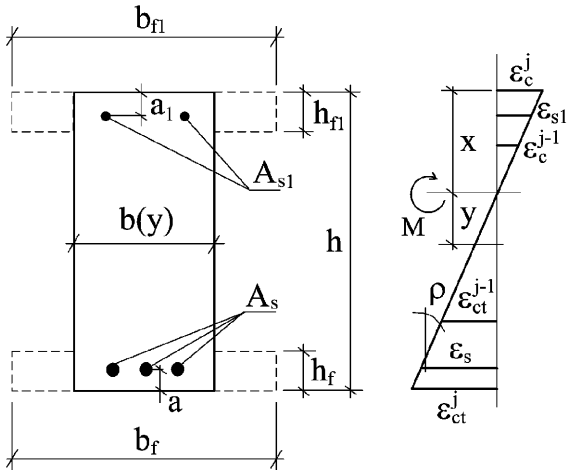

Fig. 1 RC beam cross section and strain compatibility

in which, M_c, M_{ct}, M_{s1}, M_s are the internal bending moments about a neutral axis; F_c, F_{ct}, F_{s1}, F_s are the internal forces; M is the external bending moment; ε_c^{j-1}, ε_c^j, ε_{ct}^{j-1}, ε_{ct}^j are the average strain of jth and j-1th layers; ρ is the load induced curvature; $b(y)$ is the width of cross section at a distance of y from the neutral axis (Fig. 1); $h_0 = h - a$ is an effective, while h is the overall depth of the cross section; a_1 and a are the distances between centre of gravity of compressive and tensile reinforcements to the nearest edges of the cross section; A_{s1} and A_s are the areas of reinforcement.

In Eq. (1a) and Eq. (1c), the summation symbol represents that compressive and tensile zones of the cross section are divided into the numbers of k_c and k_{ct} layers since to integrate the ramp or stepwise functions, such as $\sigma_{ct}(\varepsilon_{ct})$, $b(y)$.

2.3 Material models

To describe the compression in concrete, the linear stress strain relation including the elasto-plastic effects is applied

$$\sigma_c(\varepsilon_c) = \nu\varepsilon_c E_c \tag{2}$$

where $\nu = E_c^{sec}/E_c$ is the coefficient of elasto-plasticity for concrete in compression; E_c and E_c^{sec} are Young's tangent and secant moduli for concrete.

In general, the coefficient ν nonlinearly depends on increasing intensity of loading. When the member is subjected to bending, it is necessary to determine the character of the stress strain diagram. Following the code SNiP 1989 methodology, the coefficient ω is adopted to determine the diagram shape of concrete in compression. Hence, when loading begins the compressive zone of RC member behaves similarly to elastic material, and $\omega \approx 0.5$, $\nu \approx 1$ can be assumed. With increasing intensity of loading, plastic deformation occurs and stress strain diagram becomes similar to a rectangle, then the coefficient ω is tending to 1, while $\nu \to f_c/(E_c\varepsilon_{cR})$ (where f_c and ε_{cR} are ultimate compressive strength and the respective strain).

It is well-known that the tensile stiffness of the cracked reinforced concrete section between the consecutive cracks is higher than the stiffness of pure reinforcing steel. This property called tension

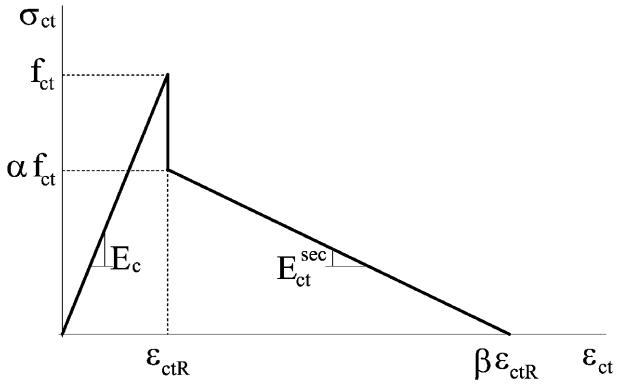

Fig. 2 Average stress strain diagram of tensile concrete

stiffness let us model by using the elementary smeared crack approach (Fig. 2). Hence, an ascending branch of the stress strain diagram simulates the behavior of the pre-cracked section while the unloading branch in the diagram accumulates tension stiffening effects, reflecting crack formation, the behavior of tensile concrete between cracks and reinforcement slipping:

$$\sigma_{ct}(\varepsilon_{ct}) = \begin{cases} \varepsilon_{ct}E_c, & \varepsilon_{ct}E_c \le f_{ct} \\ \alpha f_{ct} - E_{ct}^{sec}(\varepsilon_{ct} - \varepsilon_{ctR}), & \varepsilon_{ctR} < \varepsilon_{ct} < \beta\varepsilon_{ctR} \\ 0, & \varepsilon_{ct} \ge \beta\varepsilon_{ctR} \end{cases} \tag{3}$$

where:

$$E_{ct}^{sec} = \frac{\alpha f_{ct}}{\varepsilon_{ctR}(\beta - 1)} \tag{4}$$

$$\varepsilon_{ctR} = \frac{f_{ct}}{E_c} \tag{5}$$

in which, f_{ct} and ε_{ctR} are tensile strength and cracking strain of concrete (Fig. 2); α and β are the parameters that integrally control the tension stiffening effect (Fig. 2).

In the analysis, the elastic stress strain relations in both tension and compression zones are assumed for the reinforcement.

3. The proposed method

For the solution of the system of Eq. (1) relying on the material models, the following stages of deformational behavior of tension zone of RC members can be distinguished:

- The *pre-cracking* stage when the condition $\varepsilon_{ct} \le \varepsilon_{ctR}$ is valid;
- The *pure tension stiffening* stage when the condition $\varepsilon_{ctR} < |\rho(h-x)| \le \beta\varepsilon_{ctR}$ is satisfied;
- The *partially tension stiffening* stage is over the range $\varepsilon_{ctR} < |\rho y| \le \beta\varepsilon_{ctR} \wedge |\rho(h-x)| > \beta\varepsilon_{ctR}$;
- The *fully cracked* stage, when tensile concrete is neglected.

In the next sections, the non linear relations between internal forces/moments and respective stiffness will be considered.

3.1 Internal moments and respective stiffness

At the beginning of the pre-cracking stage the moment-curvature segment is essentially a straight line defining elastic behavior of RC section. This stage is complete at the initiation of the first flexural crack when the concrete deformation in extreme tensile fibre reaches its ultimate tensile deformation ε_{ctR}. The formula of the moment of cracking M_{cr} which corresponds to the end of pre-cracking stage is simply obtained from Eq. (1) integrating Eq. (1a) over the range of 0 and ε_{ctR}:

$$M_{cr} = \rho_{cr} E_c I_{cr} \tag{6}$$

where:

$$\rho_{cr} = \frac{\varepsilon_{ctR}}{h - x_{cr}} \tag{7}$$

$$I_{cr} = I_{cr}^c + n_c I_{cr}^s \tag{8}$$

$$I_{cr}^c = \frac{1}{3}\nu(bx_{cr}^3 + A_{f1}(3x_{cr}(x_{cr} - h_{f1}) + h_{f1}^2)) + \frac{1}{3}\left(b(h - x_{cr})^3 + \frac{A_f}{h_f}((h - x_{cr})^3 - (h - x_{cr} - h_f)^3)\right) \tag{8a}$$

$$I_{cr}^s = A_{s1}(x_{cr} - a_1)^2 + A_s(h_0 - x_{cr})^2 \tag{8b}$$

Here, ρ_{cr}, I_{cr} are the curvature and the transformed inertia moment corresponding to the end of pre-cracking stage, while I_{cr}^c, I_{cr}^s are the inertia moments for concrete and reinforcements about the neutral axis; $A_{f1} = (b_{f1} - b)h_{f1}$ and $A_f = (b_f - b)h_f$ are the areas of compressive and tensile flanges of cross section, respectively; b is the width of beam web while b_{f1}, b_f, h_{f1}, h_f are width and depth of the flanges (Fig. 1), when $b = b_{f1} = b_f$ we have rectangular cross section; $n_c = E_s/E_c$ is the modular ratio for compressive concrete and reinforcement.

The location of the neutral axis x_{cr} is defined as the roots for force balance in system Eq. (1):

$$x_{cr} = x_{cr}^{1,2} = \frac{-A_{cr} \pm \sqrt{A_{cr}^2 + 2b(\nu - 1)S_{cr}}}{b(\nu - 1)} \tag{9}$$

where A_{cr} and S_{cr} are the transformed area and the first moment of transformed area about the top surface of the cross section including coefficient ν.

Let us consider the pure tension stiffening stage. Suppose that tensile flanges of RC cross section are subjected to deformations of a descending branch of tensile concrete diagram. The internal moments Eqs. (1a)-(1b) corresponding to this stage may be obtained as:

$$M_c = \frac{\nu E_c}{\rho^2}\left(b\int_0^{x\rho} \varepsilon_c^2 d\varepsilon_c + (b_{f1} - b)\int_{(x - h_{f1})\rho}^{x\rho} \varepsilon_c^2 d\varepsilon_c\right) \tag{10}$$

$$M_{ct} = \frac{b}{\rho^2}\left(E_c\int_0^{\varepsilon_{ctR}} \varepsilon_{ct}^2 d\varepsilon_{ct} + \int_{\varepsilon_{ctR}}^{(h-x)\rho} \varepsilon_{ct}(\alpha f_{ct} - E_{ct}^{sec}(\varepsilon_{ct} - \varepsilon_{ctR}))d\varepsilon_{ct}\right) + \frac{b_f - b}{\rho^2}\int_{(h-x-h_f)\rho}^{(h-x)\rho} \varepsilon_{ct}(\alpha f_{ct} - E_{ct}^{sec}(\varepsilon_{ct} - \varepsilon_{ctR}))d\varepsilon_{ct} \tag{11}$$

$$M_{s1} + M_s = \rho E_s((x - a_1)^2 A_{s1} + (h_0 - x)^2 A_s) \tag{12}$$

and the internal forces Eqs. (1c-d) expressed as follows:

$$F_c = \frac{\nu E_c}{\rho}\left(b\int_0^{x\rho} \varepsilon_c d\varepsilon_c + (b_{f1}-b)\int_{(x-h_{f1})\rho}^{x\rho} \varepsilon_c d\varepsilon_c \right) \tag{13}$$

$$F_{ct} = \frac{1}{\rho}\left(b\left(E_c \int_0^{\varepsilon_{ctR}} \varepsilon_{ct} d\varepsilon_{ct} + \int_{\varepsilon_{ctR}}^{(h-x)\rho} \alpha f_{ct} - E_{ct}^{sec}(\varepsilon_{ct}-\varepsilon_{ctR}) d\varepsilon_{ct} \right) + (b_f - b)\int_{(h-x-h_f)\rho}^{(h-x)\rho} \alpha f_{ct} - E_{ct}^{sec}(\varepsilon_{ct}-\varepsilon_{ctR}) d\varepsilon_{ct} \right) \tag{14}$$

$$F_{s1} + F_s = \rho E_s((x-a_1)A_{s1} + (h_0 - x)A_s) \tag{15}$$

Substituting $\rho_{pr,stf} = \varepsilon_{ctR}\beta/[h - x_{pr,stf}]$ for ρ as well as $x_{pr,stf}$ for x in Eqs. (10-12) and inserting these substitutions into Eq. (1), we obtain the bending moment specifying the end of the pure tension stiffening stage, when the deformation at extreme tensile fibre reaches its ultimate tensile value $\beta\varepsilon_{ctR}$:

$$M_{pr,stf} = \rho_{pr,stf} E_c I_{pr,stf} \tag{16}$$

where:

$$I_{pr,stf} = I^c_{pr,stf} + I^{ct}_{pr,stf} + n_c I^s_{pr,stf} \tag{17}$$

$$I^c_{pr,stf} = \nu\left(\omega\omega_1 b x^3_{pr,stf} + A_{f1}\left(x^2_{pr,stf} - \frac{x_{pr,stf} h_{f1}}{2\omega} + \omega_1 \omega_f h^2_{f1} \right) \right) \tag{17a}$$

$$I^{ct}_{pr,stf} = \frac{b(h - x_{pr,stf})^3}{3\beta^3}\left(1 + n_{ct}\left(\frac{\beta(\beta^2 - 3)}{2} + 1 \right) \right) +$$

$$A_f n_{ct}\left(\left(h - x_{pr,stf} - \frac{h_f}{2} \right)(h - x_{pr,stf}) - \frac{(h - x_{pr,stf})^3 - (h - x_{pr,stf} - h_f)^3}{3h_f} \right) \tag{17b}$$

$$I^s_{pr,stf} = A_{s1}(x_{pr,stf} - a_1)^2 + A_s(h_0 - x_{pr,stf})^2 \tag{17c}$$

in which, $I_{pr,stf}$ the transformed inertia moment of cross section about the neutral axis specifying the end of pure tension stiffening stage consists of the inertia moments $I^c_{pr,stf}, I^{ct}_{pr,stf}, I^s_{pr,stf}$ for compressive and tensile concrete zones and for reinforcement; $\omega, \omega_1, \omega_f$ are the coefficients depending on the shape of the diagram for concrete in compression: for the triangular shape, $\omega = 1/2$, $\omega_1 = 2/3$, $\omega_f = 1/2$, while for the rectangular shape, $\omega = 1$, $\omega_1 = 1/2$, $\omega_f = 0$; $n_{ct} = E^{sec}_{ct}/E_c$ is the ratio between the secant and tangent Young's moduli of tensile and compressive concrete.

The location of the neutral axis $x_{pr,stf}$ is obtained as the roots of Eq. (1) using Eqs. (13-15) for force balance:

$$x_{pr,stf} = x^{1,2}_{pr,stf} = \frac{-A_{pr,stf} \pm \sqrt{A_{pr,stf}{}^2 + 4b\left(\omega\nu - \frac{1}{2\beta^2}(1 + n_{ct}(\beta - 1)^2) \right) S_{pr,stf}}}{2b\left(\omega\nu - \frac{1}{2\beta^2}(1 + n_{ct}(\beta - 1)^2) \right)} \tag{18}$$

$$A_{pr,stf} = bh\left(\frac{1}{\beta^2}(1 + n_{ct}(\beta - 1)^2) \right) + \nu A_{f1} + n_{ct} A_f + n_c(A_s + A_{s1}) \tag{19}$$

$$S_{pr,\,stf} = bh^2\frac{1+n_{ct}(\beta-1)^2}{2\beta^2} + \nu\omega_f A_{f1}h_{f1} + n_{ct}A_f\left(h-\frac{h_f}{2}\right) + n_c(A_s h_0 + A_{s1}a_1) \tag{20}$$

where, $A_{pr,\,stf}$ and $S_{pr,\,stf}$ are the transformed area and the first moment of transformed area about the top surface of the cross section specifying the end of pure tension stiffening stage.

Now, let us consider the partially tension stiffening stage. At this stage, the depth of assertion of the tensile deformations rapidly vanishes tending to almost negligible values under the increasing of bending moment. Let us omit the tensile deformations for RC beam flanges. Hence, the internal moments from Eqs. (10-12) and forces of Eqs. (13-15) can be applied to this stage, while M_{ct} and F_{ct} are rewritten as:

$$M_{ct} = \frac{b}{\rho^2}\left(E_c\int_0^{\varepsilon_{ctR}}\varepsilon_{ct}^2 d\varepsilon_{ct} + \int_{\varepsilon_{ctR}}^{\beta\varepsilon_{ctR}}\varepsilon_{ct}(\alpha f_{ct} - E_{ct}^{sec}(\varepsilon_{ct}-\varepsilon_{ctR}))d\varepsilon_{ct}\right) \tag{21}$$

$$F_{ct} = \frac{b}{\rho}\left(E_c\int_0^{\varepsilon_{ctR}}\varepsilon_{ct} d\varepsilon_{ct} + \int_{\varepsilon_{ctR}}^{\beta\varepsilon_{ctR}}\alpha f_{ct} - E_{ct}^{sec}(\varepsilon_{ct}-\varepsilon_{ctR})d\varepsilon_{ct}\right) \tag{22}$$

Finally, the inertia moment about the neutral axis specifying the fully cracked stage $I_{f,\,cr}$ may be obtained from Eq. (17) substituting 0 for $I_{pr,\,stf}^{ct}$, while the location of the neutral axis is derived by substituting 0 for $\frac{1}{2\beta^2}(1+n_{ct}(\beta-1)^2)$ in Eq. (18):

$$x_{f,\,cr} = x_{f,\,cr}^{1,2} = \frac{-A_{f,\,cr}\pm\sqrt{A_{f,\,cr}^{\;2}+4b\omega\nu S_{f,\,cr}}}{2b\omega\nu} \tag{23}$$

$$A_{f,\,cr} = \nu A_{f1} + n_c(A_s + A_{s1}) \tag{24}$$

$$S_{f,\,cr} = \nu\omega_f A_{f1}h_{f1} + n_c(A_s h_0 + A_{s1}a_1) \tag{25}$$

where $A_{f,\,cr}$ and $S_{f,\,cr}$ are the transformed area and the first moment of transformed area about the top surface of the section specifying the stage of full cracking.

As can be seen from Eq. (23), under increasing bending moment M, the location of the neutral axis remains constant. The fully cracked section stage is complete when M reaches the ultimate bending moment $M_u = \rho_u E_c I_{f,\,cr}$. The latter is determined by the ultimate curvature of RC beam ρ_u that specifies the failure mode because of concrete crushing or collapse because of steel bars breaking.

3.2 Solution

In general, the explicit solution in terms of radicals for polynomial Eq. (1) by using Eqs. (10-15) for pure tension stiffening stage, or substituting Eq. (21) and Eq. (22) instead Eq. (11) and Eq. (14), respectively, for partially stiffening stage, do not exist since the degree of a polynomial in the neutral axis is six. In order to eliminate this restriction, the linear approximation between the location of the neutral axis and bending moment is adopted:

$$x = \begin{cases} x_{pr,\,stf} + (x_{cr} - x_{pr,\,stf})\dfrac{M_{pr,\,stf} - M}{M_{pr,\,stf} - M_{cr}}, & M_{cr} \le M \le M_{pr,\,stf} \\ x_{f,\,cr} + (x_{pr,\,stf} - x_{f,\,cr})\dfrac{M_u - M}{M_u - M_{pr,\,stf}}, & M_{pr,\,stf} < M \le M_u \end{cases} \tag{26}$$

Hence, the moment-curvature equation for pure tension stiffening stage of RC beam may be obtained from the moment balance in Eq. (1) using Eqs. (10-12) as:

$$M = \left(1 + 3n_{ct}\left(\frac{1}{3} - \frac{\beta}{2}\right)\right)\frac{E_c \varepsilon_{ctR}^3 b}{3\rho^2} + E_c J_{pr,\,stf}\rho + E_{ct}^{sec}\beta\varepsilon_{ctR}S_{pr,\,stf}^{ct} \tag{27}$$

where:

$$J_{pr,\,stf} = J_{pr,\,stf}^{c} - J_{pr,\,stf}^{ct} + n_c J_{pr,\,stf}^{s} \tag{28}$$

$$J_{pr,\,stf}^{ct} = \frac{n_{ct} b (h-x)^3}{3} + A_f n_{ct}\left(\frac{(h-x)^3 - (h-x-h_f)^3}{3h_f}\right) \tag{28a}$$

$$S_{pr,\,stf}^{ct} = \frac{1}{2}b(h-x)^2 + A_f\left(h - x - \frac{h_f}{2}\right) \tag{29}$$

Here, $S_{pr,\,stf}^{ct}$ is the first moment of tensile concrete area about the neutral axis specifying the pure tension stiffening stage, $J_{pr,\,stf}$ is the transformed inertia moment of tensile concrete region about the neutral axis specifying to the stage of pure tension stiffening; $J_{pr,\,stf}^{c}, J_{pr,\,stf}^{s}$ are the inertia moments of the compressive concrete zone and reinforcement calculated by Eq. (17a) and Eq. (17c), respectively, substituting x for $x_{pr,\,stf}$; $J_{pr,\,stf}^{ct}$ is the transformed inertia moment for the tensile concrete zone.

The moment-curvature equation for the partially tension stiffening stage is obtained from Eq. (1) by using Eq. (10), Eq. (12) and Eq. (21):

$$M = \left(1 + n_{ct}\left(\frac{\beta(\beta^2 - 3)}{2} + 1\right)\right)\frac{E_c \varepsilon_{ctR}^3 b}{3\rho^2} + E_c J_{pt,\,stf}\rho \tag{30}$$

where;

$$J_{pt,\,stf} = J_{pr,\,stf}^{c} + n_c J_{pr,\,stf}^{s} \tag{31}$$

in which, $J_{pt,\,stf}$ is the transformed inertia moment about the neutral axis specifying the stage of partial tension stiffening.

The first term on the right side of cubic equations Eq. (27) and Eq. (30) expresses the non linear relation between the moment and the curvature due to the tension stiffening, while the other terms produce the linear increments. In terms of classical procedures for the solution of the polynomials, Eq. (27) has one real and two complex roots since a discriminant is positive while all roots in Eq. (30) are real since a discriminant is negative.

Finally, the solution of the equations Eq. (27) and Eq. (30) is generalized in terms of an effective moment of inertia J^{eff} and expressed as:

$$\rho = \frac{M}{E_c J^{eff}}, \quad J^{eff} > 0, \quad J^{eff} \in \mathbf{R} \tag{32}$$

Hence, the effective moment of inertia for RC beam is defined by the following relationships:

$$J^{eff} = \begin{cases} J^{eff}_{pr,\,stf}, & M_{cr} < M \le M_{pr,\,stf} \\ J^{eff}_{pt,\,stf}, & M_{pr,\,stf} < M \le M_u \end{cases} \tag{33}$$

where:

$$J^{eff}_{pr,\,stf} = J^{eff\ 1,\,2,\,3}_{pr,\,stf} = \begin{cases} \dfrac{3MJ_{pr,\,stf}}{(S^{ct}_{pr,\,stf}E^{sec}_{ct}\beta\varepsilon_{ctR} - M)((\text{sign}\ r_{pr,\,stf})2\cos(\varphi_{pr,\,stf}/3) - 1)} \\ \dfrac{3MJ_{pr,\,stf}}{(S^{ct}_{pr,\,stf}E^{sec}_{ct}\beta\varepsilon_{ctR} - M)((\text{sign}\ r_{pr,\,stf})2\cos(\varphi_{pr,\,stf}/3 + 2\pi/3) - 1)} \\ \dfrac{3MJ_{pr,\,stf}}{(S^{ct}_{pr,\,stf}E^{sec}_{ct}\beta\varepsilon_{ctR} - M)((\text{sign}\ r_{pr,\,stf})2\cos(\varphi_{pr,\,stf}/3 + 4\pi/3) - 1)} \end{cases} \tag{33a}$$

$$J^{eff}_{pt,\,stf} = J^{eff\ 1,\,2,\,3}_{pt,\,stf} = \begin{cases} \dfrac{3J_{pt,\,stf}}{2\cos(\varphi_{pt,\,stf}/3) + 1} \\ \dfrac{3J_{pt,\,stf}}{2\cos(\varphi_{pt,\,stf}/3 + 2\pi/3) + 1} \\ \dfrac{3J_{pt,\,stf}}{2\cos(\varphi_{pt,\,stf}/3 + 4\pi/3) + 1} \end{cases} \tag{33b}$$

in which:

$$\cos(\varphi_{pr,\,stf}) = -(\text{sign}\ r^3_{pr,\,stf}) - \frac{9\left(1 + 3n_{ct}\left(\frac{1}{3} - \frac{\beta}{2}\right)\right)E^3_c J^3_{pr,\,stf}\varepsilon^3_{ctR}b}{(\text{sign}\ r^3_{pr,\,stf})2J_{pr,\,stf}(S^{ct}_{pr,\,stf}E^{sec}_{ct}\beta\varepsilon_{ctR} - M)^3} \tag{33c}$$

$$\cos(\varphi_{pt,\,stf}) = 1 - \frac{9\left(1 + n_{ct}\left(\frac{\beta(\beta^2 - 3)}{2} + 1\right)\right)J^2_{pt,\,stf}E^3_c\,\varepsilon^3_{ctR}b}{2M^3} \tag{33d}$$

$$r_{pr,\,stf} = \frac{S^{ct}_{pr,\,stf}E^{sec}_{ct}\beta\varepsilon_{ctR} - M}{E_c J_{pt,\,stf}} \tag{33e}$$

$$r_{pt,\,stf} = \frac{-M}{E_c J_{pt,\,stf}} \tag{33f}$$

Here, $J^{eff}_{pr,\,stf}$ and $J^{eff}_{pt,\,stf}$ are the effective moments of inertia specifying the stages of pure tension stiffening and partial tension stiffening; while sign $q = q/|q|$, $q \neq 0$, where q is any algebraic expression.

The influence of the adopted the linear approximation between the acting moment M and the location of the neutral axis x using Eq. (26) on the moment-curvature diagram for different strength grades of concrete and reinforcement ratios μ has been investigated by comparing theoretical results determined by Eq. (32) with those solved numerically (Fig. 3). The numerical moment-curvature diagrams were obtained by solving a system non linear Eq. (1) taking into account material models

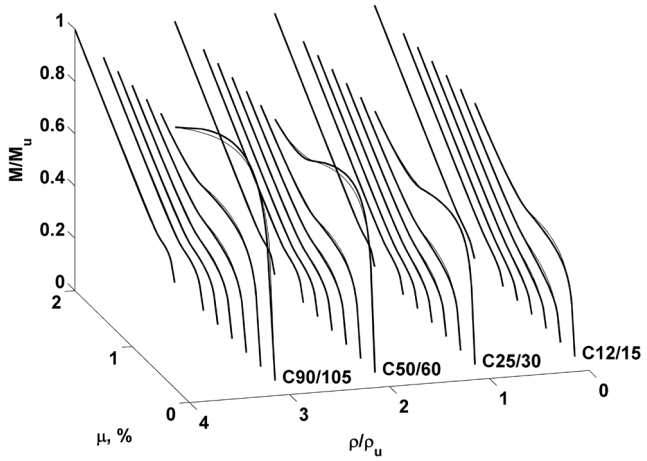

Fig. 3 The comparative graphs of dimensionless moment-curvature functions vs reinforcement ratios: numerical (bold line), method (thin line)

presented in Section 2.3. A genetic algorithm technique (see Simbirkin and Balevičius 2004) has been used to find all possible solutions of the considered non linear equations.

The comparative graphs depicted in Fig. 3 show that the numerical solution and the proposed expressions Eqs. (32-33) relying on the approximation Eq. (26) are in good agreement for the beams with reinforcement $\mu > 0.7\%$ in the both pure and partially tension stiffening stages of deformability RC members. For small reinforcement ratios, i.e., $\mu > 0.7\%$ the proposed method also provides a reasonable approximation: the relative difference between the numerical and proposed solutions are by about ±3-18% for pure tension stiffening stage, while for partially tension stiffening stage these differences are less that 2%. The presented moment-curvature diagrams (Fig. 3) have been computed for an actual experimental beam (see Nemirovskyi and Kochetkov 1969) taking into account material parameters described in Section 4.

4. Experimental verification of the method

Experimental verification of the method proposed is performed by comparing analytical and test values of the moment-curvature/deflections as well as the moment-neutral axis functions of cracked RC members in pure bending. In such a way, the proposed approach is approved for the extensive range of loading levels and different reinforcement ratios of beams. The deflections, f, have been computed by Mohr's integral relying on the variable moment of inertia $J(z)$ along the entire span z ranging from the inertia moment of transformed section specifying the pre-cracked stage to the effective moment of inertia Eq. (33). The code methods (i.e., prEN 2001, ACI 1999, SNiP 1989) corresponding to the different levels of empirical complexity have been also employed in comparative analysis.

Let us briefly describe physical properties of concrete which were implemented in the method. The governing parameter β controlling the effects of tension stiffening has been investigated by various researchers (e.g., Lin and Scordelis 1975, Schnobrick 1985, Bazant and Oh 1984, etc.) particularly in shear or tension tests using its range within 5 and 20. A comprehensive study of β

evaluation for RC elements was made by (Kaklauskas 2004) deriving average stress-strain relation of cracked tensile concrete from RC beam tests in bending (Kaklauskas 1999) using the technique described in (Kaklauskas and Ghaboussi 2001). Thus, despite of the fact that various parameters affect the character of tensile stress-strain relation, a quantitative dependence between the length of the unloading branch and the reinforcement ratio was established in (Kaklauskas 2004):

$$\beta = \begin{cases} 7.12\mu^2 - 27.6\mu + 32.8, & \mu < 2\% \\ 5, \quad \text{othervise} \end{cases} \tag{34}$$

In Eq. (34), the reinforcement ratio μ calculated by formula $\mu = \frac{A_s + A_{s1}}{bh_0} 100$ [%]. Based on the present state of knowledge, the parameter α in Eq. (3) was assumed to be 0.7.

According to the regulations of the code (SNiP 1989), the coefficient of elasto-plasticity for concrete in compression, ν, was taken to be 0.85 and additionally multiplied by the averaging factor 0.9, taking into account the uneven development of concrete strain in compression along the entire of span, if the cracking occurs. When the intensity of loading σ_c/f_c reaches 0.6 (where σ_c is the stress at extreme compressive fibre of RC cross section, and f_c is 150 × 150 mm prism strength), the rectangular shape of stress-strain diagram was assumed, taking into account that $\nu = 0.4$.

The experimental data of 62 beams reported in literature (Nemirovskyi and Kochetkov 1969, Figarovskyi 1962, Artemiev 1959, Guscha 1968) and used in developing the SNiP code (see Mulin *et al.* 1970) were also used in the present comparative analysis. All RC beams were subjected to four-point bending with a long pure bending zone (equal to 1/3 of the span) to avoid the shear effect on the beam deflections. The main characteristics of RC cross sections are presented in Table 1. As can be seen from this table, the tests represent a wide range of average concrete compressive strengths and reinforcement ratios yielded by extremely low (μ = 0.16%) and relatively high (μ = 1.63%) values.

Fig. 4 presents the diagrams of moment curvature and neutral axis comparing theoretical and experimental values (Nemirovskyi and Kochetkov 1969). As can be seen, theoretical moment-curvature diagrams predicted by Eq. (32) are in good agreement with those obtained in experiments for reinforcement ratio ranging from 0.43 to 1.51%. For slightly reinforced beams i.e., BII-1 and BI-1 the less accuracy is achieved. The linear approximation of the neutral axis vs bending moments Figs. 4(c),(d) can also be considered acceptable.

Comparative graphs for the values of the bending moment and deflections calculated by the proposed method and the testing (Figarovskyi 1962) values are shown in Fig. 5. All beams of series III had a rectangular section, while series IV was made as T section with the flanges in the tensile zone. As can be seen in Fig. 5, the theoretically obtained deflection values are in a reasonable

Table 1 Main characteristics of RC beams

Author of experiment	Total No.	150×150 cube strength, MPa	Steel yield strength, MPa	h, mm	b, mm	μ, %
Nemirovskyi	10	48.9-55.9	640-730	402-413	142-150	0.20-1.51
Figarovskyi	33	9.6-32.7	374-632	248-254	80-180	0.16-1.63
Artemiev	15	17.0-48.6	813-1062	250-264	176-187	0.99-1.12
Guscha	4	27.3-36.4	664-999	306-312	133-162	0.28-1.18

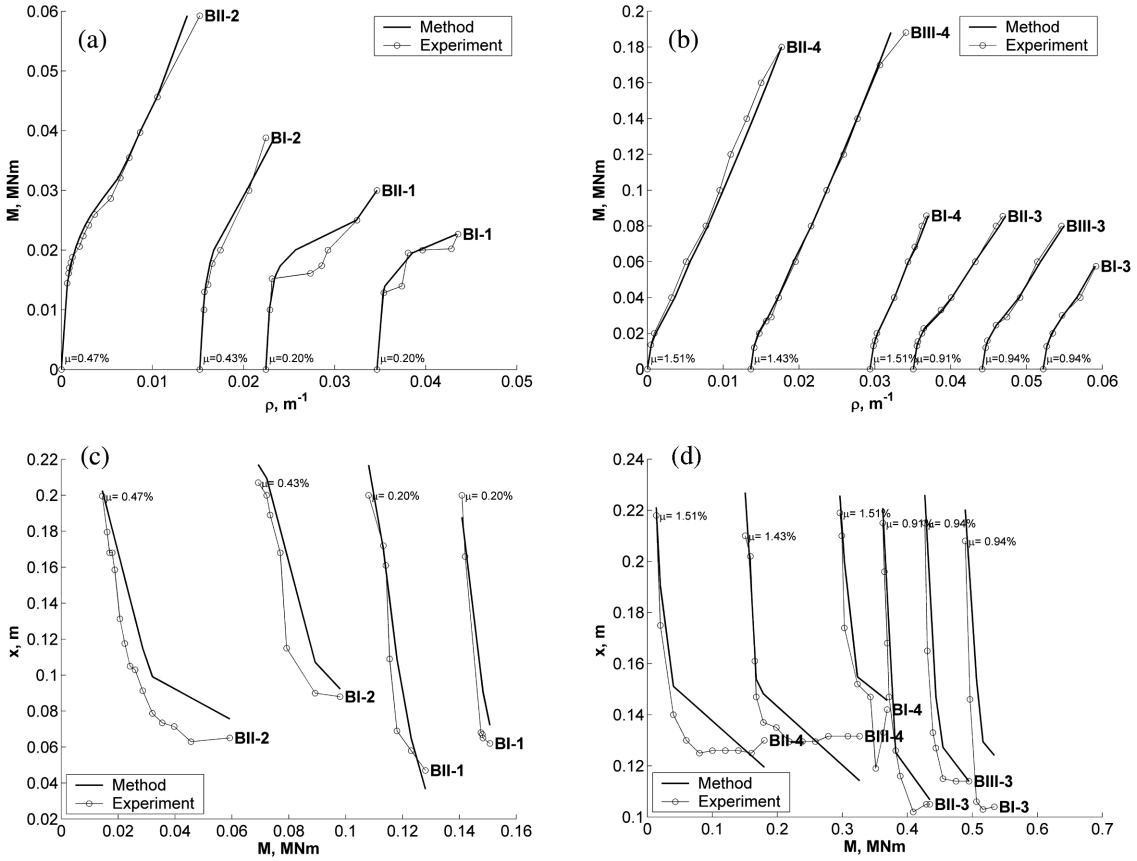

Fig. 4 Experimental and calculated curvatures (a,b) and the location of the neutral axis (c,d) vs the bending moments

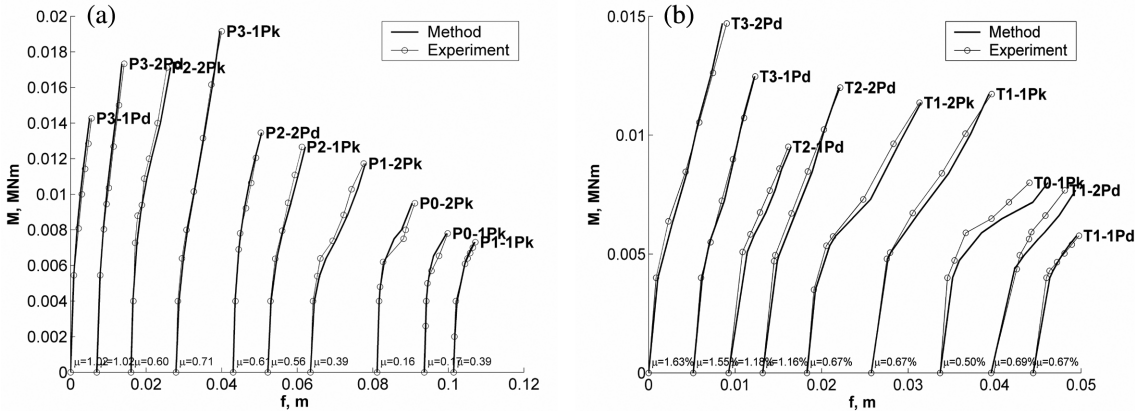

Fig. 5 Experimental and calculated beam deflections: a) rectangular cross section; b) inverted T cross section

agreement with those obtained experimentally for both rectangular and inverted T cross sections. The measured deflections for slightly reinforced T0-1Pk and T1-2Pd beams are less than theoretical.

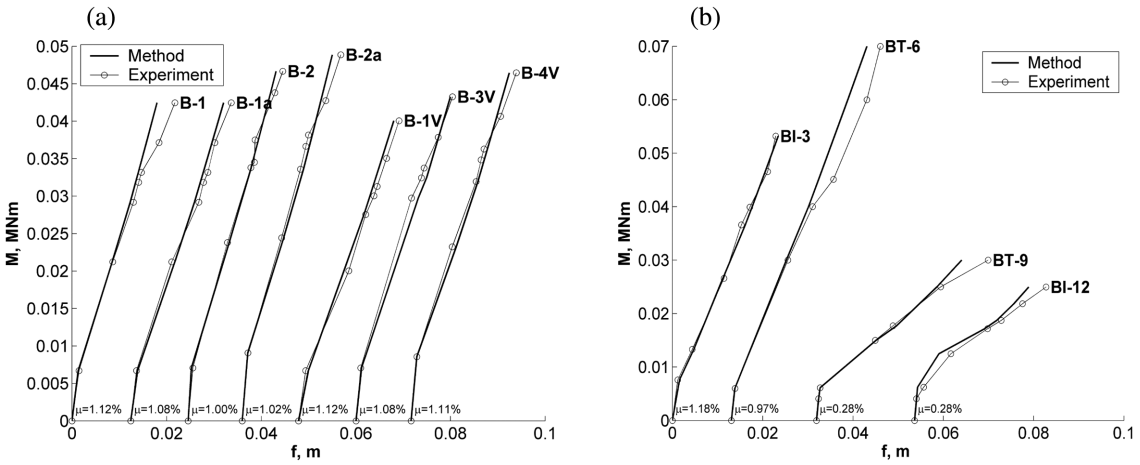

Fig. 6 Experimental and calculated beam deflections: (a) (Artemiev 1959) tests, (b) (Guscha 1968) tests

Table 2 Mean values and the coefficient of variation for relative deflections $f_{th}/f_{\exp}$

Author of experiment	ACI		prEN		SNiP		Method	
	Mean	*CV*	Mean	*CV*	Mean	*CV*	Mean	*CV*
Nemirovskyi	0.87	0.292	0.89	0.280	0.84	0.287	0.97	0.192
Figarovskyi	1.09	0.265	1.26	0.298	0.99	0.226	1.11	0.178
Artemiev	1.01	0.184	0.94	0.262	0.97	0.109	0.99	0.115
Guscha	0.88	0.324	0.84	0.259	0.92	0.208	0.95	0.179
Total:	1.00	0.274	1.05	0.335	0.96	0.223	1.04	0.183

It can be explained by the fact that a conservative theoretical assumption that tensile flanges of the beam cross section work only on a descending branch of the stress-strain diagram for pure tension stiffening stage was adopted while, for the partially tension stiffening stage, the influence of cracked tensile concrete on beam flanges was ignored completely.

Fig. 6 presents moment deflection diagrams for theoretical and experimental values (Artemiev 1959, Guscha 1968) obtained for normally (μ~1%) and slightly (μ = 0.28%) reinforced cross sections. Note, the moment-deflection behaviour was considered in the current analysis up to 0.8-0.9M_u in testing (Guscha 1968) for beams series BI-3, BT-9, BI-12.

Summarising the presented comparative analysis it should be noted that the pure tension stiffening stage occurring in slightly reinforced members can spread throughout cracking even up to failure. At this stage, the cracks develop spontaneously, suddenly reducing effective stiffness and the behavior of block of tensile concrete between the consecutive cracks, and reinforcement slippage (integrally modeled by the descending branch of stress-strain diagram of tensile concrete) has non linear effect on the deflections. The normally reinforced concrete elements usually work in both stages of partial tension stiffening and the full cracking, while the pure tension stiffening stage occurs if the acting moment is slightly higher than the moment of cracking M_{cr}. At the end of the stage of partial tension stiffening, the crack depths as well as effective stiffness remain approximately constant values under the increasing bending moment. The obtained results have also

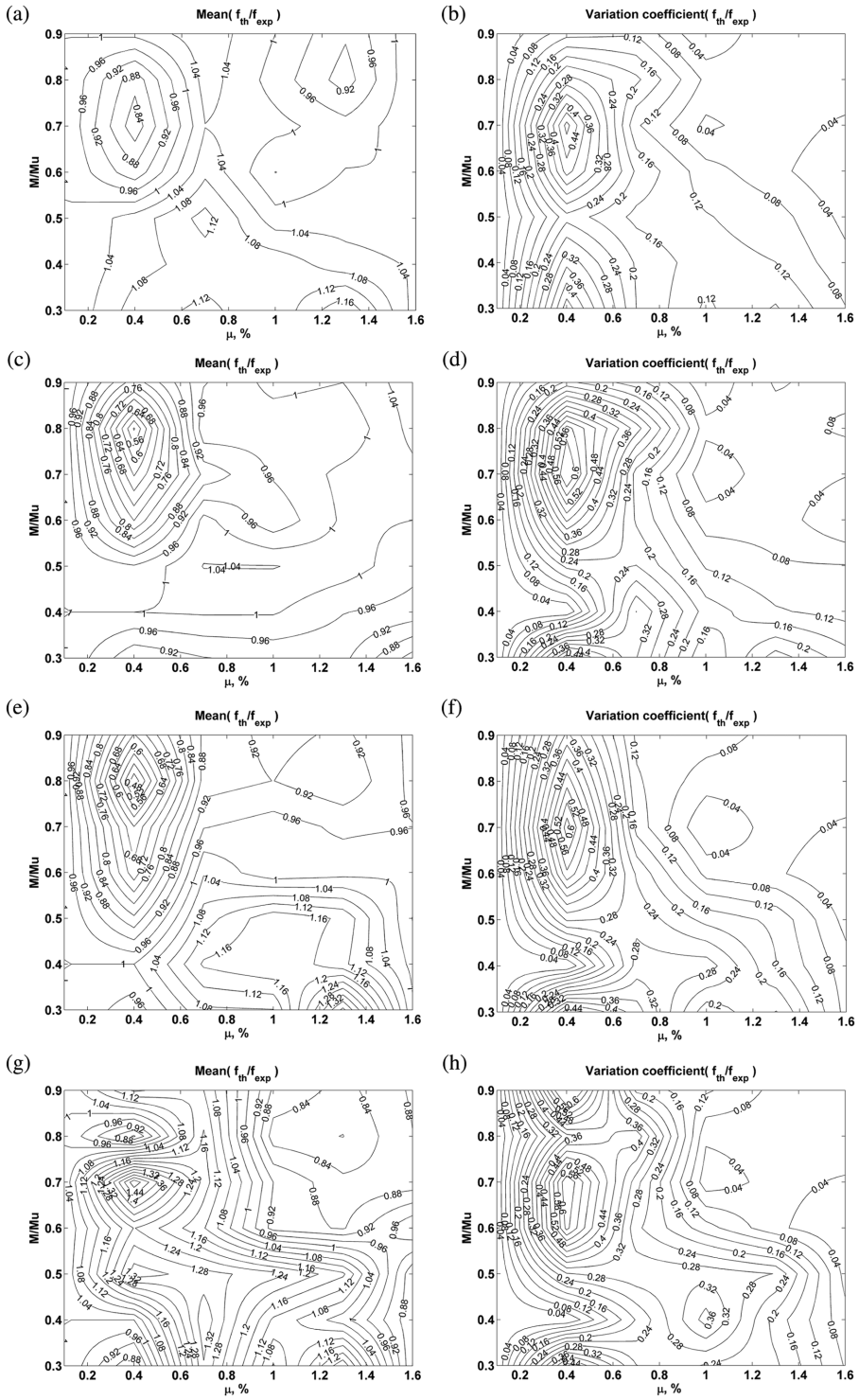

Fig. 7 Contour isolines of the mean and variation coefficient for f_{th}/f_{exp} functions: (a),(b) by proposed method, (c),(d) by code SNiP 1989, (e),(f) by code ACI 1999, (g), (h) by code prEN 2001

shown that for beams with the reinforcement ratio higher than 1.5% the tension stiffening effect could be completely ignored in calculations. The statistical data of the theoretical and experimental deflections of 62 beams are presented in Table 2.

These results (Table 2) show that, in terms of average of relative deflections f_{th}/f_{exp}, all theoretical predictions calculated by the proposed, code SNiP 1989, ACI 1999 and prEN 2001-based methods varying over the range of 0.96 and 1.04 and can be treated as sufficiently accurate. On the contrary, a less accuracy has been obtained in terms of f_{th}/f_{exp} variation; in particular, for the considered deflections sample more rigorous predictions have been achieved by the proposed method (the coefficient of variation - 18.3%), relatively accurate predictions have been made by SNiP 1989 (var. coeff. - 22.3%) and ACI 1999 (var. coeff. - 27.4%) code methods, while code prEN 2001 method gave unsatisfactory results (var. coeff. 33.5%).

The next step of analysis is related to the detailed statistical assessment and generalization of the results of relative theoretical and experimental deflections distinguished by different beam reinforcement ratios and relative moment M/M_u levels. The smoothed contour isolines of the mean and the variation coefficient functions are depicted in Fig. 7.

These graphs (Fig. 7) clearly show common tendencies and the variation bounds of the considered theoretical predictions. For the beams with small reinforcement ratio ($\mu < 0.7\%$) at the levels of the bending moments over the range of 0.5-0.9M_u the displacement predicted by the method proposed differs from their experimental values averagely over the range 0.84-1, while two code SNiP 1989 and ACI 1999 methods give rather conservative predictions ranging from 0.56 to 0.92. On the contrary, the code prEN 2001 overestimates theoretical deflections by 1.04 to 1.44 times. The distribution of the variation coefficient indicates similar tendencies. In particular, this coefficient grows from 4% to 0.44%, for the proposed method and by about 60%, for all considered code approaches. Increase in the coefficient of variation for the moment levels of (0.8-0.9)M_u can be attributed to the increased plastic strains in reinforcement steel and the compressive concrete (particularly for low-concrete grades) at advanced stress-strain states, which might be not very accurately assessed by theoretical predictions.

For beams with the reinforcement ratios higher than 0.7% and the bending moments over the range of 0.5-0.9M_u, the average values of f_{th}/f_{exp} ranges from 0.96 to 1.04 for the proposed method and SNiP 1989 technique, while for the codes ACI 1999 and prEN 2001 this ratio increases up to 1.16. The variation coefficient of these values reaches 4-16% for the proposed method, the code ACI 1999 and SNiP 1989 techniques, while for the code prEN 2001 this indicator is increased approximately to 24%.

The inaccurate stiffness assessment obtained by the above three code methods for slightly reinforced ($\mu < 0.7\%$) beams may be attributed to incomplete estimation of the increased tension stiffening effects of cracked flexural RC members. Besides, the service-bending moments for slightly reinforced beams may be relatively small, probably, close to, or even less than, the moment of cracking M_c and, therefore, the predictions of theoretical deflections mainly influenced by the prediction of M_c. The latter is strongly dependent on highly dispersed tensile concrete strength and can frequently be hardly controlled even experimentally. This fact also partly explains the above mentioned artificial stiffening of slightly reinforced beams. For fair treatment of statistical results concerning code methods, it should be mentioned that code-based approaches have been developed in order to correct predict RC member deflections at the service-load performance stage while deflections at other load levels are less important.

5. Conclusions

The results obtained in the present study may be generally summarised as follows.

The deformational analysis of reinforced concrete members from the initiation of the state of loading through serviceability conditions up to the almost structural failure has been performed on the basis of the constitutive laws for beam materials and classical principles of the strength of materials. The method proposed is based on the analytical derivation of the effective moment of inertia Eq. (33) relying on the smeared crack approach. The technique proposed, in a simplified complex manner, enables to take into account the non linear properties of compressive and tensile concrete, and the effects of cracking and bond (including the tension stiffening).

A statistical analysis has shown that the proposed technique is of adequate accuracy for calculated and experimental deflections data reported in literature which describes slightly, normally and highly reinforced beams. In particular, for the sample containing 62 beams, the most accurate predictions of the theoretical deflections have been achieved by the proposed method (the coefficient of variation for f_{th}/f_{exp} is 18.3%), relatively accurate predictions have been made by codes SNiP 1989 (var. coeff. 22.3%) and ACI 1999 (var. coeff. - 27.4%), while the code prEN 2001 has yielded rather poor results (var. coeff. 33.5%).

The performed analysis has also shown that artificial stiffening is significant for the three considered code methods for slightly reinforced ($\mu < 0.7\%$) beams working under the service-load performance. In particular, prEN 2001 method yielded significantly inaccurate estimates (the mean values of f_{th}/f_{exp} ranging from 1.04 to 1.44), sometimes up to 100% overestimating experimental deflections, while SNiP 1989 and ACI 1999 methodology is more conservative (the mean values of f_{th}/f_{exp} reaches 0.56); the proposed method, in this case, provide rather excellent results (mean of f_{th}/f_{exp} 0.84-1). Actually, these inaccuracies can have the crucial influence on codes-based evaluation of response of RC structures when the use of high-strength materials becomes popular worldwide resulting in longer spans and smaller cross sections. In this case, the method proposed enables us to perform more accurate deformational analysis of RC flexural members.

The proposed concept can be yet more improved for deformational analysis of RC members at loads level over the range of 0.9-1.0M_u (which is even more important for the beams with low reinforcement ratio) simply adopting Prandtl's stress-strain diagram for the steel reinforcement.

References

ACI (1999), *ACI Committee 318: Building Code Requirements for Reinforced Concrete and Commentary, ACI 318-99/ACI 318R-99*, American Concrete Institute, Michigan.

Al-Zaid, R.Z., Al-Shaikh, A.H. and Abu-Hussein, M.M. (1991), "Effect of loading type on the effective moment of inertia of reinforced concrete beams", *ACI J.*, **88**(2), 184-190.

Artemiev, V.P. (1959), "Investigation of strenght, stiffness and crack resistance of RC and PRC beams reinforced with 30X12C steel class", *Proc. of Institutions of Higher Education: Civil Engineering* 4, Novosibirsk. (in Russian).

Balevičius, R. and Simbirkin, V. (2005), "Non-linear physical relations for reinforced concrete elements under long-term loading", *Int. J. Appl. Mech. Eng.*, **10**(1), 5-20.

Bazant, Z.P. and Oh, B.-H. (1984), "Deformation of progressively cracking reinforced concrete beams", *ACI J.*, **81**(3), 268-278.

Branson, D.E. (1968), "Design procedures for computing deflection", *ACI J.*, **65**(9), 730-742.

Chan, C-M., Ning, F. and Mickleborough, N.C. (2000), "Lateral stiffness characteristics of tall reinforced concrete buildings under service loads", *The Structural Design of Tall Buildings*, **9**(5), 365-383.
de Borst, R. (2002), "Fracture in quasi-brittle materials: A review of continuum damage-based approaches", *Engng. Fracture Mech.*, **69**, 95-112.
Figarovskyi, V.V. (1962), "Experimental investigation of stiffness and cracking of RC flexural members subjected to short- and long-term loadings", PHD Thesis, Moscow. (in Russian).
Gilbert, R.I. (1983), "Deflection calculations for reinforced concrete beams", *Civil Engineering Transactions*, **CE25**(2), 128-134.
Guscha, Yu.P. (1968), "Investigation of flexural RC members under elasto-plastic behavior of reinforced bars", PHD Thesis, Moscow. (in Russian).
Kaklauskas, G. (1999), "A new stress-strain relationship for cracked tensile concrete in flexure", *J. Civil Eng. Management (Statyba)*, **5**(6), 349-356.
Kaklauskas, G. and Ghaboussi, J. (2001), "Stress-strain relations for cracked tensile concrete from RC beam tests", *J. Struct. Engrg.*, ASCE, **127**(1), 64-73.
Kaklauskas, G. (2004), "Flexural layered deformational model of reinforced concrete members", *Magazine of Concrete Research*, **56**(10), 575-584.
Kwak, H.G. and Kim, S-P. (2002), "Nonlinear analysis of RC beams based on moment-curvature relation", *Comput. Struct.*, **80**, 615-628.
Lin, C.S. and Scordelis, A.C. (1975), "Nonlinear analysis of RC shell of general form", *J. Struct. Div.*, ASCE, **101**(3), 523-538.
Mendis, P.A. and Darval, P.I. (1988), "Stability analysis of softening frames", *J. Struct. Eng.*, ASCE, **114**(5), 1057-1072.
Mulin, N.M., Artemiev, V.P., Belobrov, I.K., Guzeev, Ye.A., Krasovskaya, G.M., Petrova, K.V. and Figarovskyi, V.V. (1970), "Substantiation of deformational analysis by new code project", *Proc. of Institution of Higher Educations: Civil Engineering 8*, Novosibirsk. (in Russian).
Nemirovskyi, Ya.M. and Kochetkov, O.I. (1969), "The influence of tensile and compressive concrete on the deformational behavior of flexural RC members after cracking", *Deformational Peculiarities of Plain and Reinforced Concretes and Computer Based Estimation of their Influence on the Behavior of Structures*, A.A. Gvozdev and S.M. Krylov Editors, NIIZHB, Moscow, 38-76. (in Russian).
Ngo, D. and Scordelis, A.C. (1967), "Finite element analysis of reinforced concrete beams", *ACI J.*, **64**(3), 152-163.
Ning, F., Mickleborough, N.C. and Chan, Ch-M. (2001), "Service load response prediction of reinforced concrete flexural members", *Struct. Eng. Mech.*, **12**(1), 1-16.
Pietruszczak, S. and Mroz, Z. (1981), "Finite element analysis of deformation of strain softening materials", *Int. J. Numer. Meth. Eng.*, **17**, 327-334.
Prakhya, G.K.V. and Morley, C.T. (1990), "Tension stiffening and moment-curvature relations for reinforced concrete elements", *ACI J.*, **87**(5), 597-605.
prEN (2001), *EuroCode 2: Design of Concrete Structures, prEN 1992–1*, European Committee for Standardization, Brusselles.
Rashid, Y.R. (1968), "Analysis of prestressed concrete pressure vessels", *Nucl. Engng. Design*, **7**(4), 334-344.
Razaqpur, A.G. and Isgor, O.B. (2003), "Rational method for calculating deflection of continuous FRP R/C beams", *ACI J.*, **210** (special publications), 191-208.
Rozenbliumas, A. (1966), "Calculation of reinforced concrete structures in consideration of tensile stress of concrete", *Investigation of Reinforced Concrete Structures 1,* Vilnius. 3-32. (in Russian).
Schnobrick, W.C. (1985), "Role of finite element analysis of reinforced concrete structures", *Proc. of the Seminar on Finite Element Analysis of Reinforced Concrete Structures*, Tokyo, May.
Scott, R.H. and Beeby, A.W. (2005), "Long-term tension-stiffening effects in concrete", *ACI J.*, **102**(1), 31-39.
Simbirkin, V. and Balevičius, R. (2004), "Long-term strength and deformational analysis of reinforced concrete columns", *J. Civil Eng. Management*, **10**(1), 67-75.
Sluys, L.J. and de Borst, R. (1996), "Failure in plain and reinforced concrete – an analysis of crack width and crack spacing", *Int. J. Solids Struct.*, **33**(20-22), 3257-3276.
SNiP (1989), *Concrete and Reinforced Concrete Structures. Design Code SNiP 2.03.01-84*, Gosstroy SSSR,

Moscow. (in Russian).
Suidan, M. and Schnobrich, W.C. (1973), "Finite element analysis of reinforced concrete", *J. Struct. Div.*, ASCE, **99**(10), 2109-2122.
Yost, J.R., Gross, Sh.P. and Dinehart, D.W. (2003), "Effective moment of inertia for glass fiber-reinforced polymer-reinforced concrete beams", *ACI J.*, **100**(6), 732-739.
Zalesov, A.S., Kodysh, E.N., Lemysh, L.L. and Nikitin, I.K. (1988), *Strength and Deformational Analysis of RC Structures*, Stroyizdat, Moscow. (in Russian).

Notation

A : area
I : inertia moment specifying the end of respective stages
J : inertia moment of respective stages
S : first moment of area
CV : correlation coefficient of relative deflections
E : Young's modulus
F : axial force
M : bending moment
a_1, a : distances (see Fig. 1)
b : width of web of cross section
h_0 : effective depth of cross section
h : overall depth of cross section
x : location of neutral axis
y : distance from neutral axis
k : the number of layers
n : Young's moduli ratio
q : any algebraic expression
f : deflection
f_c : compressive strength
f_{ct} : tensile strength
ρ : curvature
μ : reinforcement ratio
σ : average normal stress
ε : average strain
ε_{cR} : ultimate compressive strain of concrete
ε_{ctR} : cracking strain of concrete
ν : coefficient of elasto-plasticity of concrete in compression
ω, ω_1, ω_f : coefficients of diagram shape of concrete in compression
α, β : parameters of stress-strain relationship (see Fig. 2)

Subscripts or superscripts

c : compressive concrete
ct : tensile concrete
s : tensile steel
$s1$: compressive steel

Subscripts

cr : cracking stage
pr,stf : pure tension stiffening stage

pt,stf : partially tension stiffening stage
f,cr : fully cracked stage
u : ultimate
th : theoretical
exp : experimental
*f*1 : compressive flanges of cross section
f : tensile flanges of cross section

Superscripts

eff : effective
sec : secant
j : *j*th layer